RESEARCH PAPER

Computational Fluid Dynamics Simulation of Combustion Instability in Solid Rocket Motor : Implementation of Pressure Coupled Response Function

S. Saha and D. Chakraborty[*]

Directorate of Computational Dynamics, Defence Research and Development Laboratory, Hyderabad – 500 058, India
[*]Correspondence e-mail: debasis_cfd@drdl.drdo.in

ABSTRACT

Combustion instability in solid propellant rocket motor is numerically simulated by implementing propellant response function with quasi steady homogeneous one dimensional formulation. The convolution integral of propellant response with pressure history is implemented through a user defined function in commercial computational fluid dynamics software. The methodology is validated against literature reported motor test and other simulation results. Computed amplitude of pressure fluctuations compare closely with the literarture data. The growth rate of pressure oscillations of a cylindrical grain solid rocket motor is determined for different response functions at the fundamental longitudinal frequency. It is observed that for response function more than a critical value, the motor exhibits exponential growth rate of pressure oscillations.

Keywords: Computational fluid dynamics, solid rocket motor, propellant combustion, combustion instability, acoustics oscillation

NOMENCLATURE

A, B	QSHOD coefficients of pressure response function
$dm(\omega)$	Fluctuation of mass burn rate of propellant over mean
$dp(\omega)$	Fluctuation of propellant surface pressure over mean.
f	Acoustic frequency in the motor cavity
$\bar{m}$	Mean mass burn rate of propellant
n	Pressure index of steady state propellant burning
$\bar{p}$	Mean propellant surface pressure
$\lvert p'(t) \rvert$	Amplitude of pressure oscillation at time t
$\lvert p'_0 \rvert$	Amplitude of pressure oscillation at a time $t = 0$
$R_p(\omega)$	Pressure response function of solid propellant
$R(\tau)$	Response function in time domain
r_{b0}	Steady state burn rate of propellant
α	Net exponential growth rate of pressure fluctuation
α_{decay}	Exponential decay rate of pressure oscillations
α_s	Propellant thermal diffusivity
$\omega = 2\pi f$	Angular frequency (of fluctuation of pressure and propellant burn rate) [*rad/s*]
Ω	Non dimensional frequency

1. INTRODUCTION

Coupling of pressure response of propellant combustion with acoustics oscillation in the motor port cause 'combustion instability' which plagued the development of many solid rocket motor of aerospace applications[1]. From a linear point of view, the stability of solid rocket motor can be evaluated by combined effect of driving and damping mechanisms[2]. Driving mechanisms are mostly due to propellant burning which coupled with port acoustics tend to increase the energy of the flow disturbances. Some other interactions like wave motion in the nozzle, particulate damping, structural damping etc. tend to dissipate the energy of the flow disturbances and thus exert a stabilising influence on the motor. Thus a meaningful stability analysis of rocket motor calls for an evaluation of energy balances between energy gains and energy losses that pertained to the motor under consideration.

Efforts are continuing for the past few decades to solve the problem of combustion instability through theoretical[3,4] and experimental techniques[5,6]. Many active control methods like vortex shedding in large segmented motors[7] and neural dynamic optimisation[8] and passive control methods like Helmoholtz resonator[9], acoustics liner[10] were used to break the coupling between unsteady heat release and acoustics waves. Blomshield[1] analysed 28 motors that had experienced combustion instability and what was done to solve the problem. The cause of combustion instability is yet to be understood properly.

With the advent of powerful computer, advanced physical and chemical models, robust numerical algorithms, computational fluid dynamics (CFD) methods are increasingly applied to solve the unsteady flow field in solid rocket motors with metalised and nonmetalised propellants. Since, the hostile character of the environment inside a solid rocket motor permits only pressure measurements, numerical simulations were the best way to acquire knowledge of details of the internal flowfield. Geometric evolution of grain boundaries and performance parameters[11] are predicted, erosive burning correlations for axisymmetric geometries are extended to complex grain shapes[12,13] and accumulated slag were estimated for a large segmented rockets with submerged nozzle[14]. Nozzle damping coefficients were estimated numerically[15] for cold

flow experimental condition and a very good match between experimental and numerical results for different throat to port area ratio were obtained. The validated methodology was applied to predict the nozzle damping coefficients for a solid rocket motor with finocyl grain geometry. The role of turbulence in the motor port is also investigated by performing simulation with laminar and turbulent conditions and concluded that laminar simulation is adequate to study the acoustics resonance in the motor port.

Applications of unsteady CFD methodology in predicting the axial acoustics fluctuations in solid rocket motor are also reported in the open literature. Flandro & Jacob[16] emphasised that the motor instability is linked to the hydro-dynamic instability of the mean flow sheared regions. To predict motor flow driven instabilities, we need to use a model that has the ability to describe, in the same framework, both acoustic and vortical waves. Numerical solution of compressible Navier-Stokes equations provides the needed framework. ONERA's experience indicates that for complex geometries, simplified methods based on acoustic balance cannot give reliable results in terms of stability. Full numerical approaches must be used, in providing insight into oscillatory flow fields and must become irreplaceable tools to predict motor stability. After more than ten years of sustained CFD research in ONERA, CFD methods are available to build a detailed understanding of the instability mechanisms[17,18]. An unsteady quasi-one-dimensional flow solver with higher-order numerical solutions for simulating internal ballistics and axial acoustic fluctuations in solid rocket motors is developed by Chakravarthy[19], *et al*. The characteristic frequencies, corresponding mode shapes, and damping rates is estimated for cylindrical grain geometry. Further progress in simulation of heterogeneous propellant combustion is available in literature[20].

Guery[18] proposed a mathematical formulation to describe the unsteady mass flow rate caused due to pressure coupling effect. The same formulation is implemented in the commercial CFD software Fluent[21] through a user defined function in the present work. The developed model is validated by comparing experimental pressure data[6] of a 'whistling motor' available in literature. The methodology is also tested for a cylindrical grain SRM and the results are analysed.

2. METHODOLOGY

The pressure coupled response function is an intrinsic property of solid propellant and is measured regularly by various techniques like T-burner, rotating valve motor, etc. It is a complex number that expresses the amplitude and phase relationship between the propellant burning rate and oscillation pressure as a function of frequency. The pressure coupled response function is defined as:

$$R_p\left(\omega\right) = \frac{dm\dot{}(\omega)\big/\overline{m}}{dp(\omega)\big/\overline{p}} \qquad (1)$$

where $d\dot{m}(\omega)$ is the fluctuation of propellant mass burn rate (over a mean value of $\overline{m}$), due to pressure fluctuation of $dp(\omega)$ (over a mean value of $\overline{p}$) at angular frequency ω.

The QSHOD formulation introduced by Culick[2] using a Green's function for the linear wave equations provided an efficient way of computing the dominant Eigen modes and provide a useful mean to compute unsteady mass flow rate based on fluctuating pressure. According to QSHOD formulation, pressure response, $R_p\left(\omega\right)$ with its constant terms *n, A* and *B,* adjusted to fit experimental data of propellant combustion are as follows

$$R_p = \frac{nAB}{\lambda + \dfrac{A}{\lambda} - \left(1 + A\right) + AB}$$

where

$$\lambda = \frac{1 + \sqrt{1 + 4i\Omega}}{2}$$

and

$$\Omega = 2\pi f \left(\frac{\alpha_s}{r_{b0}^2}\right)$$

In time domain, the Eqn. (1) becomes a convolution integral

$$\dot{m}(t) = \overline{m}\left(1 + \int_0^{t_0} R(\tau)\frac{p(t-\tau) - \overline{p}}{\overline{p}}d\tau\right)$$

This mass flux formulation is implemented as inlet mass flux UDF on the propellant surface. Before switching on the UDF, the flow inside the SRM is simulated by solving three dimensional unsteady Navier Stokes equations with fixed mass flux inlet boundary condition on propellant surface till pressure values reaches a statistical steady state. Simulations were carried out in an axisymmetric geometry using density based solver with 2nd order discretisation in space and time. Once a statistical steady state is reached, the mass flux UDF implementing the pressure response is switched on and solver is run further to observe the effects.

3. RESULTS AND DISCUSSION
3.1 Validation Case

The effect of pressure coupled response was validated against literature work carried out by Lupoglazoff & Vuillot[6]. The test case is a 'whistling motor' in which the instabilities are driven by self exciting vortex-shedding oscillations. The propellant is filled from head end till the middle and terminated by a 45° backward facing step producing vortex shading. The test geometry is shown in Fig 1. Comparison of R_p distribution assumed for the present simulation (red curve, with $n = 0.5$, $A = 4.5867$, $B = 0.6152$, and $\alpha_s/r_{b0}^2 = 8.1278*10^{-4}$ [s]) and those obtained from *T* Burner test (green dots) and R_p assumed for simulation in literature (blue curve) is shown in Fig. 2. The time domain equivalent of response function used for present simulation is shown in Fig. 3. The simulation domain was discretised with quadrilateral cells with 21 K nodes, as shown in Fig. 4. Nonmetalised solid propellant is used in the experiment of whistling motor. In absence of any data on propellant, a typical non aluminised propellant was assumed with a flame temperature of 2800 K (to achieve the desired longitudinal frequency) for the simulation. Figures 5(a) and 5(b) show a qualitative comparison of vorticity for present simulation and simulation by Lupoglazoff & Vuillot[6]. The vortex distribution is similar. Three vortex structures are
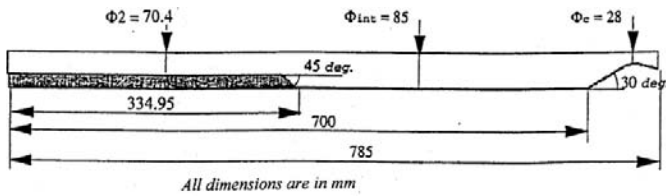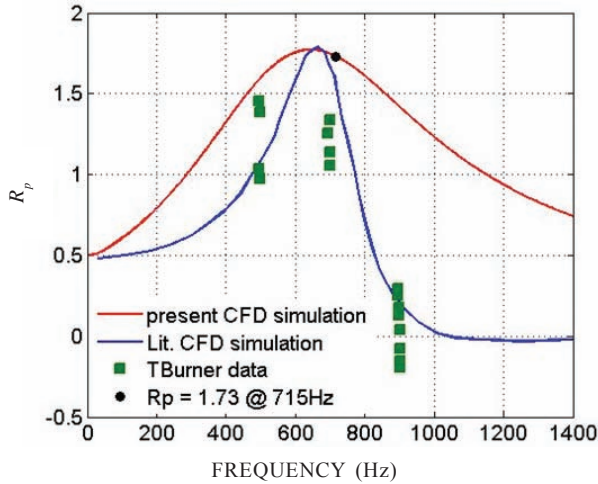
Figure 1. Geometry of motor considered for validation[10].

Figure 2. Comparison of R_p distribution assumed for the present simulation (red curve), obtained from T Burner test (green dots), and R_p assumed for simulation in literature (blue curve).
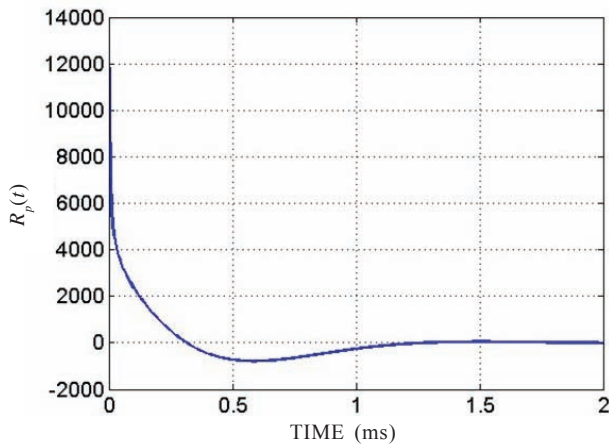

Figure 3. Response function in time domain $R_p(t)$ distribution obtained from $R_p(\omega)$ used for the present simulation.
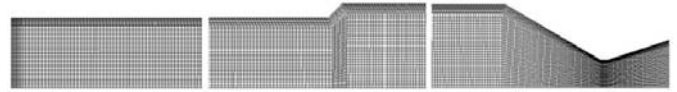

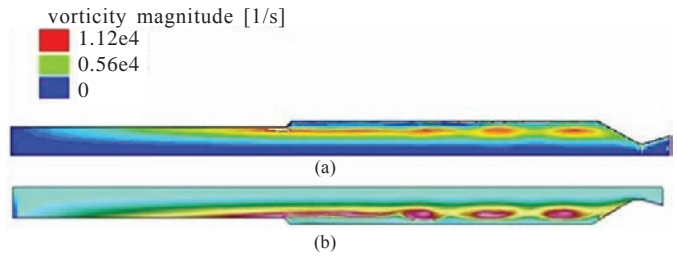Figure 4. Grid distribution for validation case.

Figure 5. Vorticity plot: (a) for present simulation and (b) for simulation in literature.
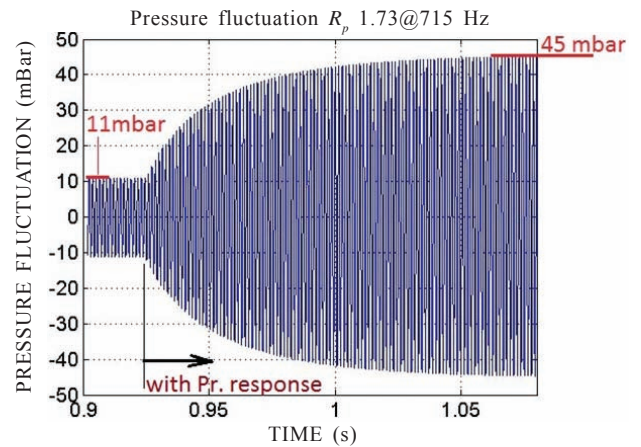

Figure 6. Increase in amplitude of pressure oscillations due to activation of pressure response function at time = 0.925 s.

Table 1. Comparison of amplitude of oscillating pressure obtained in the present simulation with literature CFD simulation and test

	Present CFD simulation	Literature CFD simulation	Test data
Without pressure response function	11 mbar	12.7 mbar	-
With pressure response function	45 mbar	43.1 mbar	43.9 mbar

comparison to 12.7 mbar of simulation reported in literature. With pressure coupling, the present simulation predicted 45 mbar pressure oscillation, in comparison to 43.1 mbar measured in motor test and 43.9 mbar obtained from CFD simulation. A marginally higher prediction of present simulation could be because of a marginally higher R_p at 715 Hz assumed for present simulation, as can be seen in Fig. 2.

3.2 Demonstration of Combustion Instability due to Pressure Coupled Response Function

The methodology was tested on a cylindrical grain SRM shown in Fig. 7, having similar length, throat and core diameter as one of the practical SRM which had shown combustion Instability. The $R_p(\omega)$ distribution was assumed to such that
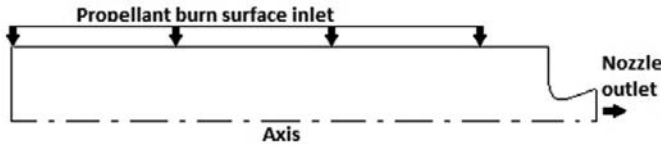
seen in both simulations at the given instant of time. These structures were observed to move downstream with time. The quantitative comparisons could not be made due to lack of information from literature. The increase in amplitude of acoustic pressure oscillations at a head end location, from 11 mbar to 45 mbar after the pressure response function was activated at time = 0.925 s, is shown in Fig 6. The frequency of computed pressure oscillations was 715 Hz as compared to 720 Hz reported[6]. The amplitudes of oscillating pressure compare well with literature simulation and test data is shown in Table 1. Without pressure coupling, the present simulation predicted 11 mbar amplitude of pressure oscillation, in

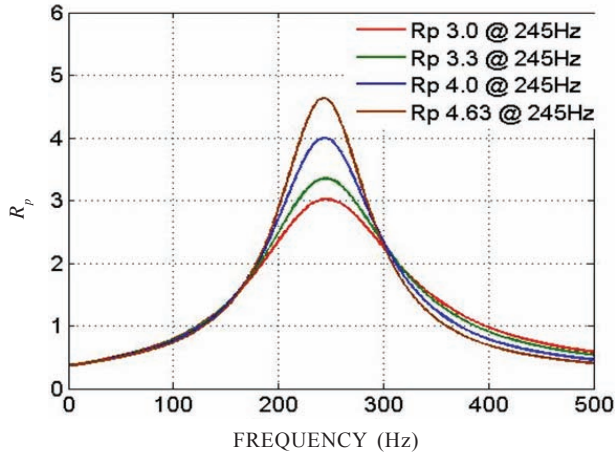**Figure 7.** Axisymmetric geometry of motor with cylindrical propellant.

Figure 8. $R_p(\omega)$ distributions for used for different simulations.

R_p = 4.63 at 245 Hz, the fundamental longitudinal frequency of the SRM. Figure 8 shows the $R_p(\omega)$ distribution for R_p = 4.63 and other values for which simulations were carried out. Axisymmetric domain was discretised with 70 K square nodes. Figure 9 plots the history of head end pressure in the motor as evolved during simulation. It is seen that starting from an almost zero value, the amplitude of pressure fluctuation grows exponentially to a maximum of about 30 bar (26 per cent of mean pressure). After the fluctuations reached a maximum value, the pressure response was turned off. The pressure fluctuations damped down. Detailed analysis of pressure history at head end at different time regime along with the growth and decay rate are shown in Fig. 10. The initial exponential growth rate of pressure fluctuation over initial pressure is shown in Fig 10(a). The exponential growth rate was found to be $\alpha = 18.2[1/s]$, where the growth rate of pressure fluctuations
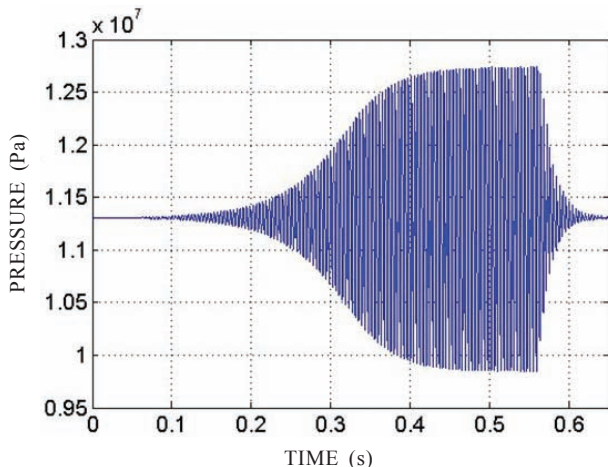

Figure 9. Head end pressure obtained for $R_p(\omega)$ distribution corresponding to R_p = 4.63 @ 245 Hz.
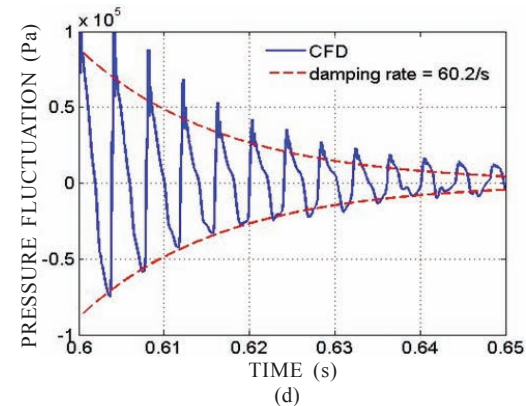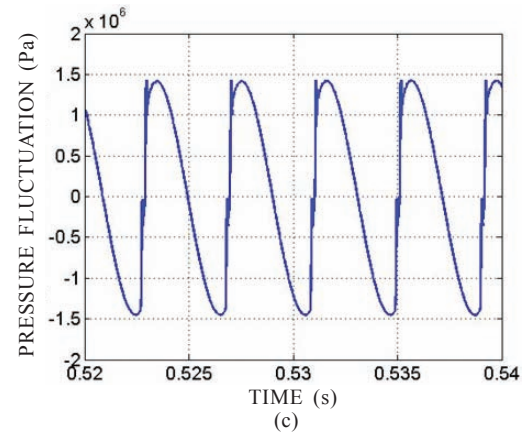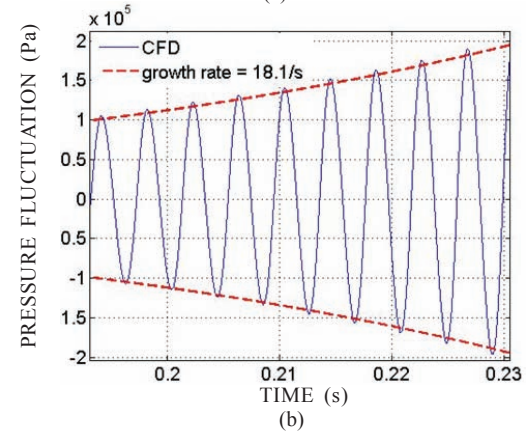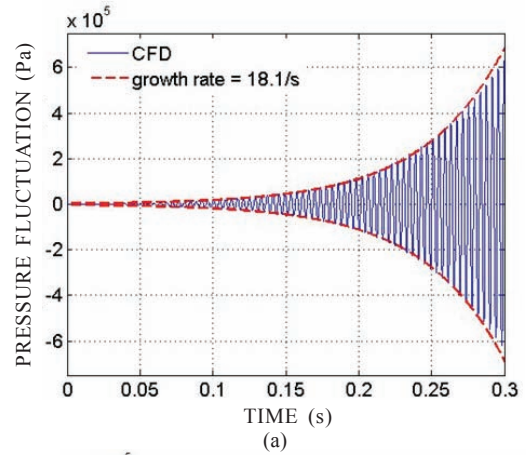

Figure 10. Different time regimes of the pressure history: (a) Initial exponential growth phase, (b) Sinusoidal nature of initial exponential growth phase, (c) Limited pressure oscillation phase, and (d) Damping phase.

α, is defined in $\left|p'(t)\right| = \left|p'_0\right| \times e^{\alpha t}$, with magnitude of pressure fluctuation, $\left|p'(t)\right|$ growing exponentially from a reference pressure fluctuation value of $\left|p'_0\right|$. Figure 10(b) shows the sinusoidal nature of growth of pressure oscillations during 0.2 to 0.23 ms. The pressure fluctuation grows to a limit where the pressure fluctuation are high enough to become sharp fronted waves, as can be seen in Fig 10(c). When the pressure response was switched off, the fluctuations starts decaying, but not sinusoidally. Therefore the damping in this case is not linear and exponential curve of $\alpha_{decay} = 60.2[1/s]$ does not fit with the decaying pressure fluctuation, as shown in Fig 10(d). To determine the damping coefficient of the motor, another simulation was carried out to introduce pressure fluctuation to about 2 bar (peak-to-peak) ensuring sinusoidal pressure fluctuation, and then switching off pressure response to simulate damping. Figure 11(a) shows the initial growth, and subsequent decay of the pressure fluctuations. The decay in this case is sinusoidal and hence an exponential decay of $\alpha_{decay} = 60.2[1/s]$ was observed, as seen in Fig 11(b).

Similar exercise was carried out with two different $R_p(\omega)$ distributions such that $R_p = 4.0$, and $R_p = 3.3$ at 245 Hz. The growth rate of pressure oscillations were found to be, $\alpha = 12[1/s]$ for $R_p = 4.0$, and $\alpha = 0[1/s]$ for $R_p = 3.3$. The data is plotted as growth rate $vs\ R_p$ at 245 Hz in Fig. 12.
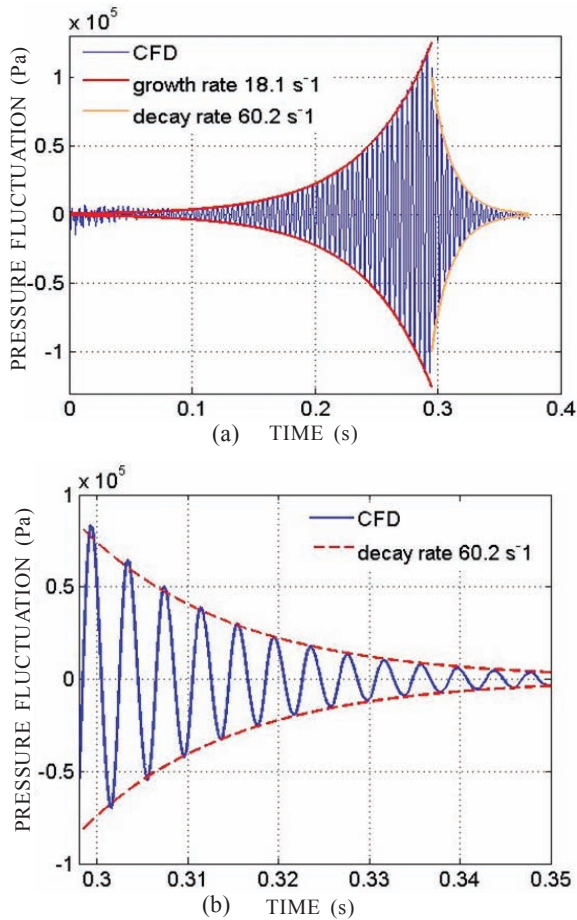

Figure 11. Demonstration of exponential damping in the cylindrical grain SRM: (a) Initial exponential growth followed by damping and (b) sinusoidal and exponential damping.
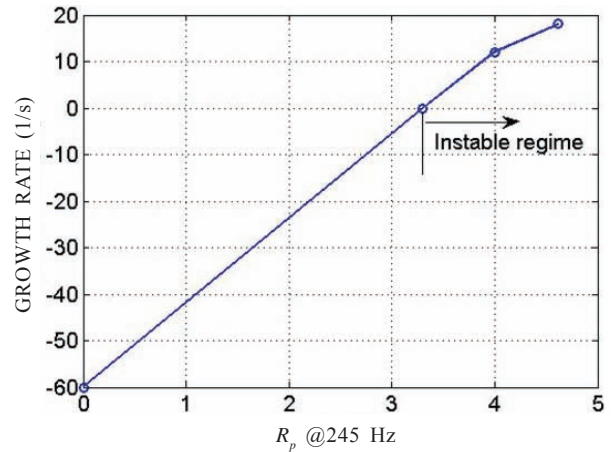

Figure 12. Growth rate vs R_p plot for the SRM, indicating instability regime of motor operation.

When pressure response is switched off, $R_p = 0$, the growth rate is negative meaning damping. From the figure it can be seen that if the propellant response has a value more than $R_p = 3.3$ at 245 Hz the cylindrical grain SRM will always show instability. At $R_p = 3.3$, the disturbances generated due to pressure response matches the damping losses and the SRM is at the verge of instability for the particular grain diameter. As the grain geometry changes with burn time, the generation and damping of disturbances changes, and the methodology will predict a range of R_p values (for each grain geometry) at which the generation just exceeds damping and predict instability of SRM. Given the proper pressure response of propellant, the CFD methodology can then predict the time of occurrence of instability in SRMs. The time instant at which the propellant R_p exceeds the critical R_p for the grain geometry, instability is expected to set in.

4. CONCLUSIONS

A user defined function modelling the pressure response of solid propellant combustion, is implemented as inlet mass flux boundary condition on propellant surface in commercial software to model of solid propellant burning. Experimental data of a 'whistling motor' available in literature is taken as test case for validation and computed pressure at the head end match well with experimental data. The methodology was applied on a cylindrical grain SRM, resulting in an exponential rise in pressure oscillations, thereby demonstrating combustion instability due to pressure response of propellant. The methodology also predicted the minimum pressure response value at which generation of disturbance due to pressure coupling just exceeds damping of disturbance in SRM, to predict occurrence of 'linear instability' in SRM.

REFERENCES

1. Blomshield, F.S. Lessons learned in solid rocket combustion instability. AIAA Paper 2007-5803.
2. Culick, F.E.C. Unsteady motions in combustion chambers for propulsion systems. 2006, RTO AGARDograph AG-AVT-039.
3. Shimada, T.; Masahisa, H.; Takakazu, M.; Takashi K.; Yosh-ikawa, T. & Yasuhiko, W. Stability analysis of

solid rocket motor combustion by computational fluid dynamics. *AIAA Journal*, 2008, **46**, 947-957.
doi: 10.2514/1.31976.

4. Ananthkrishnan, N.; Deo, S. & Culick, F.E.C. Reduced-order modeling and dynamics of nonlinear acoustic waves in a combustion chamber. *Combust. Sci. Technol.,* 2005, **177**, 221- 247.
doi: 10.1080/00102200590900219.

5. Kuentzmann, P. & Laverdant, A. Experimental determination of the response of a solid propellant to high-frequency pressure oscillation. *Res. Aerospatale,* 1984, **l 1**, 39-55.

6. Lupoglazoff, N. & Vuillot, F. Simulations of solid propellant rocket motor instability including propellant propellant combustion response. *In* the 6th International Conference on Sound and Vibration, Lyngby (Denmark), 1999. ONERA –TP-1999-133.

7. Anthoine, J. & Mettenleiter, M. Influence of adaptive control on vortex-driven instabilities in a scaled model of solid propellant motors. *J. Sound Vibration,* 2003, **206**, 1009-1046.

8. Fichera, A. & Pagano, A. Application of neural dynamic optimisation to combustion-instability control. *Applied Energy,* 2006, **83**, 253-264.

9. Zhao, D. Transmission loss analysis of a parallel coupled Helmholtz resonator network. *AIAA Journal,* 2012, **50**, 1339-1346.
doi: 10.2514/J.105145.

10. Zhong, Z. & Zhao, D. Time-domain characterisation of acoustics damping of a perforated liner with bias flow. *J. Acoustics Soc.,* 2012, **312,** 271-281.

11. Javed, A.; Iyer, A.S. & Chakraborty, D. Internal Ballistic Code for Solid Rocket Motors using Minimum Distance Function for Grain Burnback. *Def. Sci. J.* 2015, 65(3), 181-188.
doi: 10.14429/dsj.65.8304.

12. Mukunda, H.S. Extension of the universal erosive burning law to partly symmetric propellant grain geometries. *Acta Astronautica,* 2014, **93**, 176-181.
doi:10.1016/j.acta.2013.07.017

13. Javed, A. & Chakraborty, D. Universal erosive burning model performance for solid rocket motor internal ballistics. *Aerospace Sci. Technol.,* 2015, **45**, 150-153.
doi: 10.1016/j.a.st.2015.05.005.

14. Chaturvedi, A.K; Kumar, S & Chakraborty, D. Slag prediction in submerged rocket nozzle through two phase CFD simulations. *Def. Sci. J.*, 2015, **65**(2), 99.
doi: 10.14429/dsj.65.7147.

15. Javed, A. & Chakraborty, D. Damping coefficient prediction of solid rocket motor nozzle using computational fluid dynamics. *J. Propulsion Power*, 2013, **30**(1), 19–23.
doi:10.2514/1.B35010

16. Jacob, E.J. & Flandro, G.A. Thrust oscillations in large solid rocket boosters. AIAA Paper No. 2008-4601

17. Fabignon,Y.; Dupays, J.; Avalon, G.; Vuillot, F.; Lupoglazoff, N.; Casalis, G. & Michel, P. Instabilities and pressure oscillations in solid rocket motors. *Aerospace Sci. Technol.*, 2003, **7**, 191–200.
doi:10.1016/S1270-9638(02)01194-X

18. Guéry, J. Numerical modeling of internal flow aerodynamics part 2: Unsteady flows. in internal aerody-namics in solid rocket propulsion, RTO educational notes EN-023 AVT-096, AVT-VKI presentation on 27-31 May 2002 in Rhode-Saint-Genèse, Belgium.

19. Chakravarthy, V. Kalyana; Iyer, Arvind & Chakraborty, Debasis. Quasi-one-dimensional modeling of internal ballistics and axial acoustic oscillations in solid rocket motors. *J. Propulsion Power.* (Online: April 15, 2016)
doi: 10.2514/1.B35754

20. Jackson, T.L. Modeling of heterogeneous propellant combustion: A survey. *AIAA Journal*, 2012, **50**(5), 993-1006.
doi: 10.2514/1.J051585.

21. Fluent. Fluent Users Guide, (September 2006).

CONTRIBUTORS

Mr Soumyajit Saha obtained his ME (Aerospace Engineering) from Indian Institute of Science, Bengaluru. Presently, he is working as Scientist 'F' in Directorate of Computational Dynamics, DRDL, Hyderabad. His research interests are : CFD, aero-dynamics, high-speed combustion, and propulsion.
In current study, he has generated the computational grid, performed unsteady simulation, post process the results and prepared all the figures

Dr Debasis Chakraborty obtained his PhD in Aerospace Engineering from Indian Institute of Science, Bengaluru. Presently, he is working as Technology Director, Computational Dynamics Directorate, DRDL, Hyderabad. His research interests are : CFD, aerodynamics, high-speed combustion, and propulsion.
In current study, he has contributed in overall planning of the simulation, guidance of the work, review of the results and preparation of the manuscript.